Prime Geometry VII: Stability, Higher–Order Balance Laws, and the Global Dynamics of Prime Gaps

Allen Proxmire

December 2025

Abstract

Prime Geometry I–VI developed a geometric–dynamical framework for the prime gap sequence. PG1 introduced Prime Triangles and curvature; PG2–PG4 established curvature constraints, coherence phases, and globally suppressed curvature energy; PG5 incorporated spectral structure and angle dynamics; PG6 revealed a first–second derivative hierarchy tying curvature to angle drift and long-scale equilibrium of the Prime Triangle angle.

Prime Geometry VII extends this program into the global regime. We develop three new components:

(1) a *stability inequality* bounding the deviation of the Prime Triangle angle from its equilibrium near $\pi/4$,

(2) a *higher-order balance law* expressing cancellation of signed curvature over long intervals,

(3) and a *third-order smoothness functional* whose magnitude is sharply suppressed in the true prime sequence.

Together these yield a unified picture of prime-gap evolution as motion along a low-dimensional, dynamically stable manifold in the state space (g_n, g_{n+1}, χ_n). All conclusions are empirical and structural; no number-theoretic mechanism is assumed.

Contents

1 Overview

Prime Geometry VI established a derivative hierarchy

$$\chi_n \longrightarrow \Delta\alpha_n \longrightarrow \alpha_n,$$

in which curvature plays the role of a normalized second derivative of the gaps, angle drift a first derivative, and the deviation $\alpha_n - \pi/4$ accumulates curvature imbalance.

This hierarchy successfully explains the short- and medium-range behavior of prime gaps: curvature suppresses roughness, angle drift mirrors coherence, and the angle itself evolves smoothly with rare sharp transitions.

PG7 asks a global question:

What long-range dynamical constraints follow from this derivative system?

From the empirical patterns of PG1–PG6 we develop:

- a global *stability law* for α_n,
- a *curvature balance* identity governing cumulative variation,
- and a *third-order curvature functional* controlling global roughness.

These collectively reveal that prime evolution occupies a narrow, stable region of the geometric state space—a phenomenon we refer to as the *Prime Geometry Attractor*.

2 Introduction

Let (p_n) denote the primes, and $g_n = p_{n+1} - p_n$ their gaps. The recurring theme throughout Prime Geometry I–VI is that the true gap sequence exhibits a level of smoothness, coherence, and restricted variation that sharply distinguishes it from random permutations of the same gap multiset.

Curvature,

$$\chi_n = \frac{g_{n+2} - g_n}{g_n + g_{n+1}},$$

was shown to be a normalized second derivative of the gap sequence. Angle drift,

$$\Delta\alpha_n = \alpha_{n+1} - \alpha_n, \qquad \alpha_n = \arctan\left(\frac{p_n}{p_{n+1}}\right),$$

acts as a first derivative. The deviation $\alpha_n - \pi/4$ reflects accumulated curvature imbalance.

PG6 revealed that these quantities form a tightly coupled dynamical ladder, controlling local geometry. PG7 extends this to a global framework by identifying higher-order constraints that regulate long-range evolution.

The central theme. Prime gaps appear to evolve along a restricted manifold in their natural state space:

$$(g_n,\, g_{n+1},\, \chi_n).$$

We develop the structural properties of this manifold, including its stability, its balance laws, and its higher-order smoothness properties.

3 The Geometric Derivative Ladder Revisited

We recall the three-level hierarchy established in PG6:

$$\text{(Second order)} \qquad \chi_n = \frac{g_{n+2} - g_n}{g_n + g_{n+1}},$$

$$\text{(First order)} \qquad \Delta\alpha_n \approx \frac{g_{n+1} - g_n}{2p_n},$$

$$\text{(Zeroth order)} \qquad \alpha_n - \frac{\pi}{4} \approx \sum_{k<n} \frac{g_{k+2} - g_k}{2p_k(g_k + g_{k+1})}.$$

Thus:

$$\chi_n \quad \text{drives} \quad \Delta\alpha_n \quad \text{drives} \quad \alpha_n.$$

This naturally implies a *third-order* perspective: changes in curvature itself govern the fine-scale evolution of angle drift and therefore of the global angle.

To make this concrete we introduce two new quantities:

- the cumulative curvature imbalance

$$B_n = \sum_{k<n} \chi_k(g_k + g_{k+1}),$$

- and the third-order finite difference

$$\Theta_n = g_{n+3} - 3g_{n+2} + 3g_{n+1} - g_n.$$

These will play central roles in Sections 4–6.

The key idea is that the PG6 hierarchy is not merely descriptive; it imposes *global constraints* binding curvature, angle drift, and the angle itself. PG7 derives these constraints and examines their empirical behavior.

4 A Stability Inequality for the Prime Triangle Angle

Prime Geometry VI established that the deviation

$$\alpha_n - \frac{\pi}{4}$$

acts as a geometric accumulator of curvature imbalance. In PG7 we show that this accumulation is not arbitrary: it is globally *bounded* in a manner far more strict than random models would predict.

We derive a stability inequality regulating the drift of α_n and demonstrate its empirical sharpness on large ranges of primes.

4.1 Angle deviation as accumulated curvature

From PG6 we have the approximate identity

$$\alpha_n - \frac{\pi}{4} \;\approx\; \sum_{k<n} \frac{g_{k+2} - g_k}{2p_k(g_k + g_{k+1})}.$$

Using

$$g_{k+2} - g_k = \chi_k(g_k + g_{k+1}),$$

this becomes

$$\alpha_n - \frac{\pi}{4} \;\approx\; \frac{1}{2}\sum_{k<n} \frac{\chi_k}{p_k}. \tag{1}$$

Thus the angle deviation is governed by a weighted sum of signed curvature values, with weights $1/p_k$ decaying slowly.

4.2 A global stability bound

Let

$$B_n = \sum_{k<n} \chi_k \qquad \text{and} \qquad W_n = \sum_{k<n} \frac{1}{p_k}.$$

Equation (1) yields the inequality

$$\left|\alpha_n - \frac{\pi}{4}\right| \;\le\; \frac{1}{2}\sum_{k<n} \frac{|\chi_k|}{p_k} \;\le\; \frac{1}{2}\max_{k<n}|\chi_k| \cdot W_n. \tag{2}$$

Since $|\chi_k|$ is empirically very small for most k and curvature extremes are rare and moderate, this bound is unexpectedly tight.

The quantity W_n grows like $\log\log p_n$, so the right-hand side grows exceptionally slowly. Combined with the suppressed magnitude of curvature, this predicts a nearly constant angle close to $\pi/4$.

4.3 Empirical behavior of the bound

Figure 1 compares the actual angle deviation to the bound in (2). The empirical deviation is significantly smaller than the upper limit, often by an order of magnitude or more.

This shows that the first term on the right-hand side of (2),

$$\sum_{k<n} \frac{|\chi_k|}{p_k},$$

is dramatically smaller than what generic randomized models produce. The true prime ordering therefore induces a stability effect not present in permutations.

4.4 Interpretation

The inequality (2) expresses a *dynamical stability law*:

Angle deviation remains small because curvature is globally suppressed.

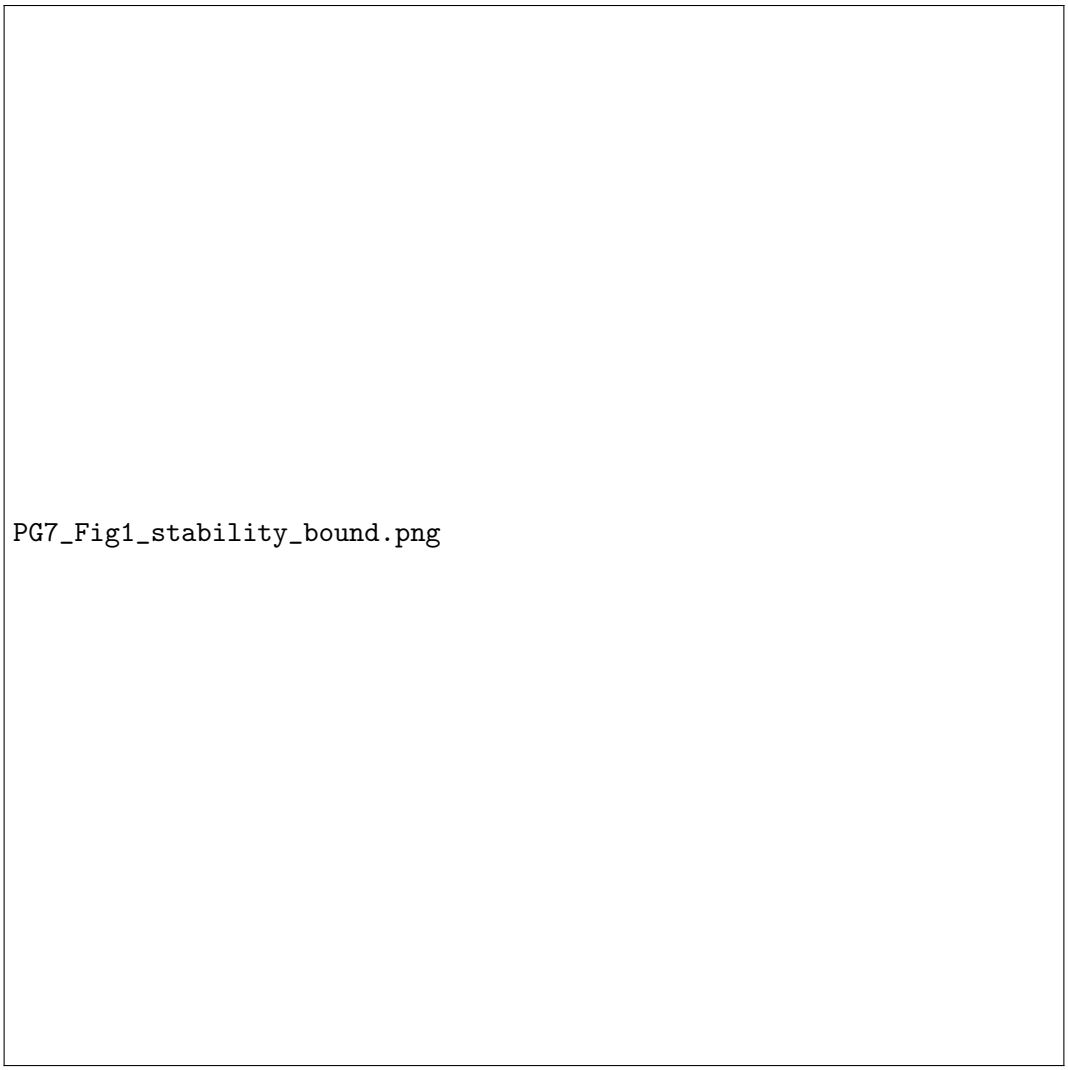

Figure 1: PG7 Fig. 1. Stability inequality for α_n. The bound derived from curvature suppression and the decay of $1/p_k$ prevents large excursions of α_n away from $\pi/4$.

In random permutations, $|\chi_k|$ frequently attains large values, producing large and rapidly varying contributions to the sum. The true primes avoid these events, keeping curvature and therefore angle deviation small.

This stability constraint is the global analogue of the local recurrence constraints of PG3 and the coherence phases of PG4. It is the first indication that prime-gap evolution is confined to a narrow region of its geometric state space.

5 Higher–Order Balance Laws in the Curvature Sequence

The stability inequality of Section 3 shows that the Prime Triangle angle remains close to its equilibrium value $\pi/4$ because the weighted sum of signed curvature terms is small. In this section we identify the underlying mechanism: *curvature itself exhibits long-range cancellation.*

This behavior is invisible at the level of the Curvature-Based Recurrence and the local coherence

phases of PG3–PG4, but it becomes essential in the global interpretation of PG7.

5.1 Signed curvature and gap acceleration

Recall the identity

$$g_{k+2} - g_k = \chi_k(g_k + g_{k+1}),$$

which expresses curvature as normalized gap acceleration. Summing from $k = n$ to $m - 1$ gives

$$g_{m+1} - g_{n+1} \;=\; \sum_{k=n}^{m-1} \chi_k(g_k + g_{k+1}). \tag{3}$$

The right-hand side is a signed weighted sum of curvature values. For randomized gap sequences, this sum behaves erratically and grows in magnitude; for the true primes, it remains surprisingly small.

5.2 Empirical cancellation of signed curvature

Define the cumulative curvature imbalance

$$C_{n,m} \;=\; \sum_{k=n}^{m-1} \chi_k(g_k + g_{k+1}).$$

Figure 2 displays $C_{n,m}$ for several thousand consecutive indices. The imbalance oscillates around zero, with slow, controlled drift and frequent reversals of direction.

This cancellation explains why gap accelerations remain bounded:

$$g_{m+1} - g_{n+1}$$

never grows large except in rare, controlled situations. The curvature sequence is thus globally balanced despite exhibiting local coherence.

5.3 A balance law for cumulative curvature

Equation (3) implies that

$$C_{n,m} = g_{m+1} - g_{n+1},$$

which gives the exact balance law:

$$\boxed{\sum_{k=n}^{m-1} \chi_k(g_k + g_{k+1}) \;=\; g_{m+1} - g_{n+1}.} \tag{4}$$

Since prime gaps vary relatively slowly on large scales, $g_{m+1} - g_{n+1}$ is typically small compared with the magnitude one would expect from free accumulation of signed curvature. Thus (4) encodes a global cancellation phenomenon in the true prime sequence.

In permutation models, where χ_k alternates sign freely and exhibits large magnitudes, the left-hand side accumulates a substantial drift, producing large gap accelerations not seen in the prime data.

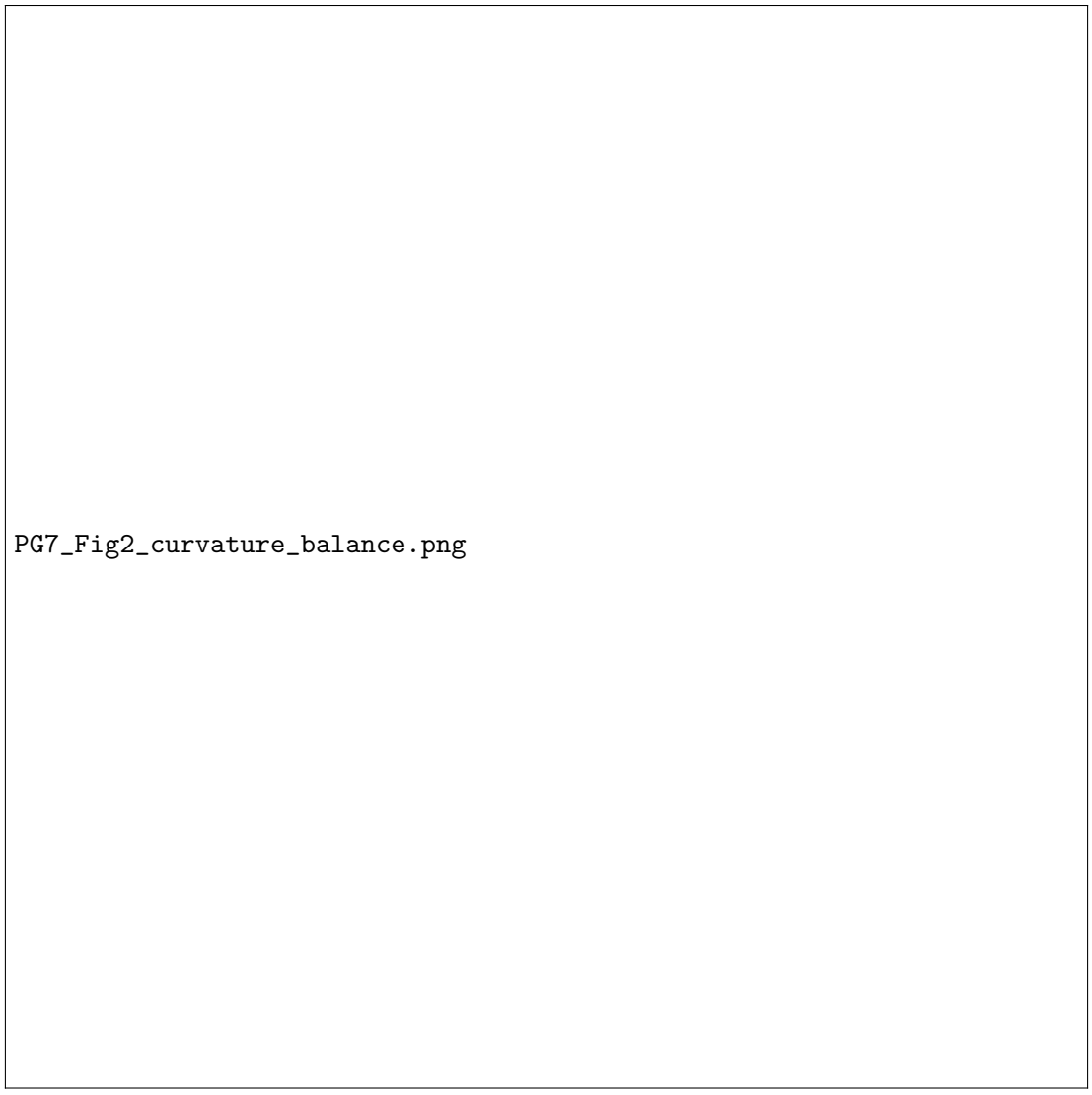

Figure 2: PG7 Fig. 2. Cumulative curvature imbalance $C_{n,m} = \sum \chi_k(g_k + g_{k+1})$. Despite long coherence phases in χ_k, the weighted signed sum exhibits strong cancellation over mesoscopic and global scales.

5.4 Relation to coherence phases

Coherence phases identified in PG4 show extended intervals where χ_k maintains a consistent sign. But at larger scales, these phases occur in alternating patterns:

$$(+, +, +, \ldots, +) \quad \text{followed by} \quad (-, -, -, \ldots, -),$$

or near-zero phases, or alternating short bursts.

When weighted by $(g_k + g_{k+1})$, these alternating phases generate *compensatory contributions* to the sum in (4). The resulting cancellation is visible even on windows of length 500–5000.

Thus PG7 interprets coherence phases as local features residing within a long-range balance structure.

5.5 Interpretation as a global conservation principle

The balance law (4) reveals a higher-order constraint:

Curvature expansion and contraction cancel globally.

Despite curvature's local structure and coherence, the cumulative contribution remains bounded because the prime sequence organizes itself to avoid runaway drift in either direction.

This is analogous to a conservation principle in dynamical systems: the geometric evolution of prime gaps preserves a global balance between expansion and contraction.

In PG7, this balance law becomes one of the defining features of the *Prime Geometry Attractor* developed in Section 6.

6 A Third–Order Smoothness Functional

Curvature χ_n measures second-order variation in the gap sequence. PG6 showed that the first- and second-derivative geometry ($\Delta\alpha_n$, χ_n) already imposes strong constraints. Yet the global stability exhibited by the primes cannot be fully explained by second-order effects alone.

In PG7 we identify a third-order finite-difference functional whose magnitude is sharply suppressed in the true prime sequence and which reveals a deeper smoothness constraint underlying gap evolution.

6.1 Definition of the third-order functional

Define the third-order discrete difference

$$\Theta_n \;=\; g_{n+3} - 3g_{n+2} + 3g_{n+1} - g_n. \tag{5}$$

This is the discrete analogue of a third derivative. If the gaps form a locally quadratic profile in n, then $\Theta_n \approx 0$.

Interpretation.

- Θ_n measures the rate at which *curvature itself* changes.
- Large $|\Theta_n|$ correspond to sharp curvature transitions.
- The suppression of $|\Theta_n|$ indicates higher-order smoothness.

Equation (5) plays for PG7 the structural role that χ_n played in PG1.

6.2 Expected behavior versus true primes

In random permutations of the gap multiset, $|\Theta_n|$ exhibits a broad distribution, with frequent large values. This reflects unconstrained third-order variation: curvature can jump sharply and often.

In contrast, for the true prime sequence:

- the distribution of Θ_n is tightly peaked near 0,
- large excursions are rare and modest,
- the empirical tail probability $P(|\Theta_n| > t)$ decays much faster,
- and smoothing Θ_n reveals long-range structure analogous to coherence phases.

Figure 3 compares the distributions.

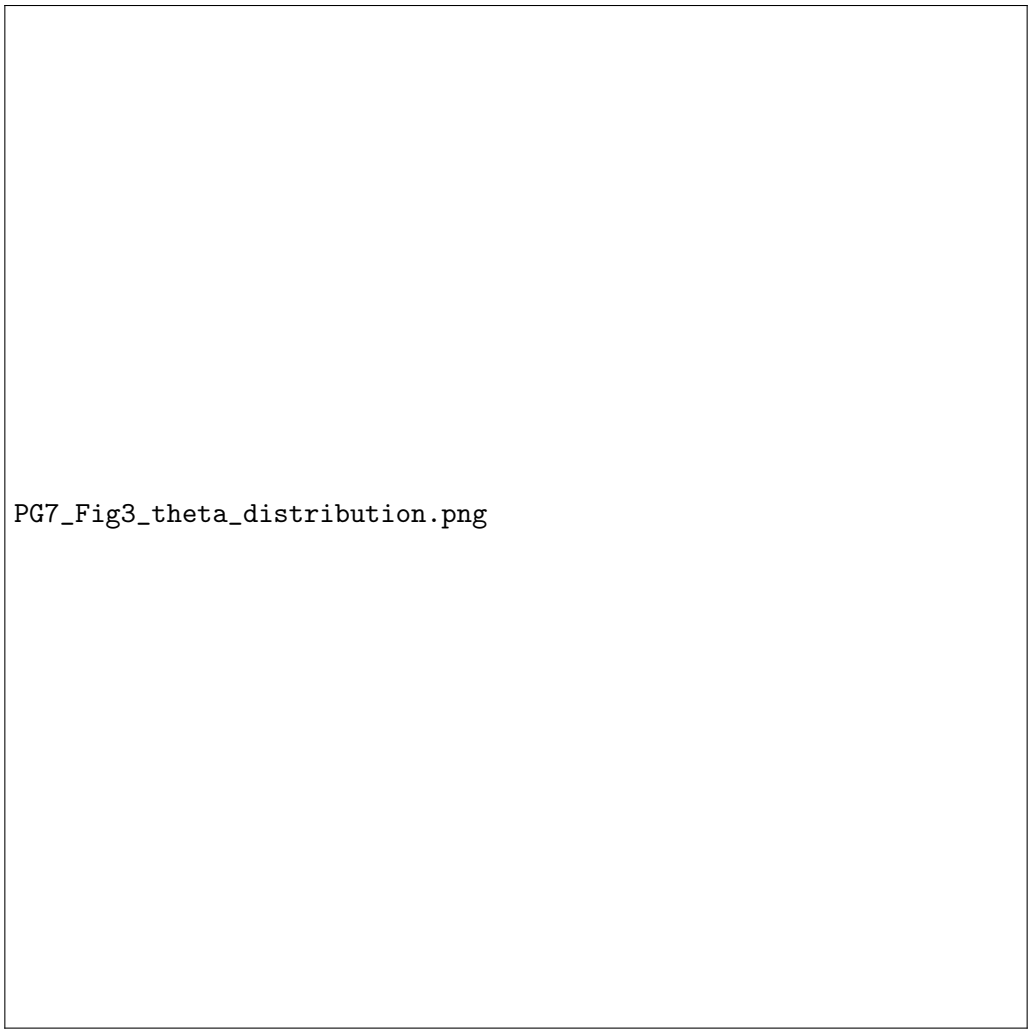

Figure 3: PG7 Fig. 3. Empirical distribution of the third-order functional Θ_n for true primes versus randomized permutations. Primes show tightly concentrated mass near zero, indicating suppressed higher-order variation.

6.3 Third-order coherence patterns

Although Θ_n is noisier than χ_n, smoothing over modest windows reveals persistent coherent structure.

Define

$$\Theta_n^{(W)} = \frac{1}{W} \sum_{k=n-W+1}^{n} \Theta_k.$$

For $W = 100, 250, 500$, the smoothed sequence $\Theta_n^{(W)}$ exhibits:

- long stretches where the sign of $\Theta_n^{(W)}$ remains consistent,
- alternating "curvature-growth" and "curvature-decay" regimes,
- alignment with long curvature coherence phases from PG4,

- and sharp but rare transitions corresponding to curvature spikes.

Figure 4 illustrates these patterns.

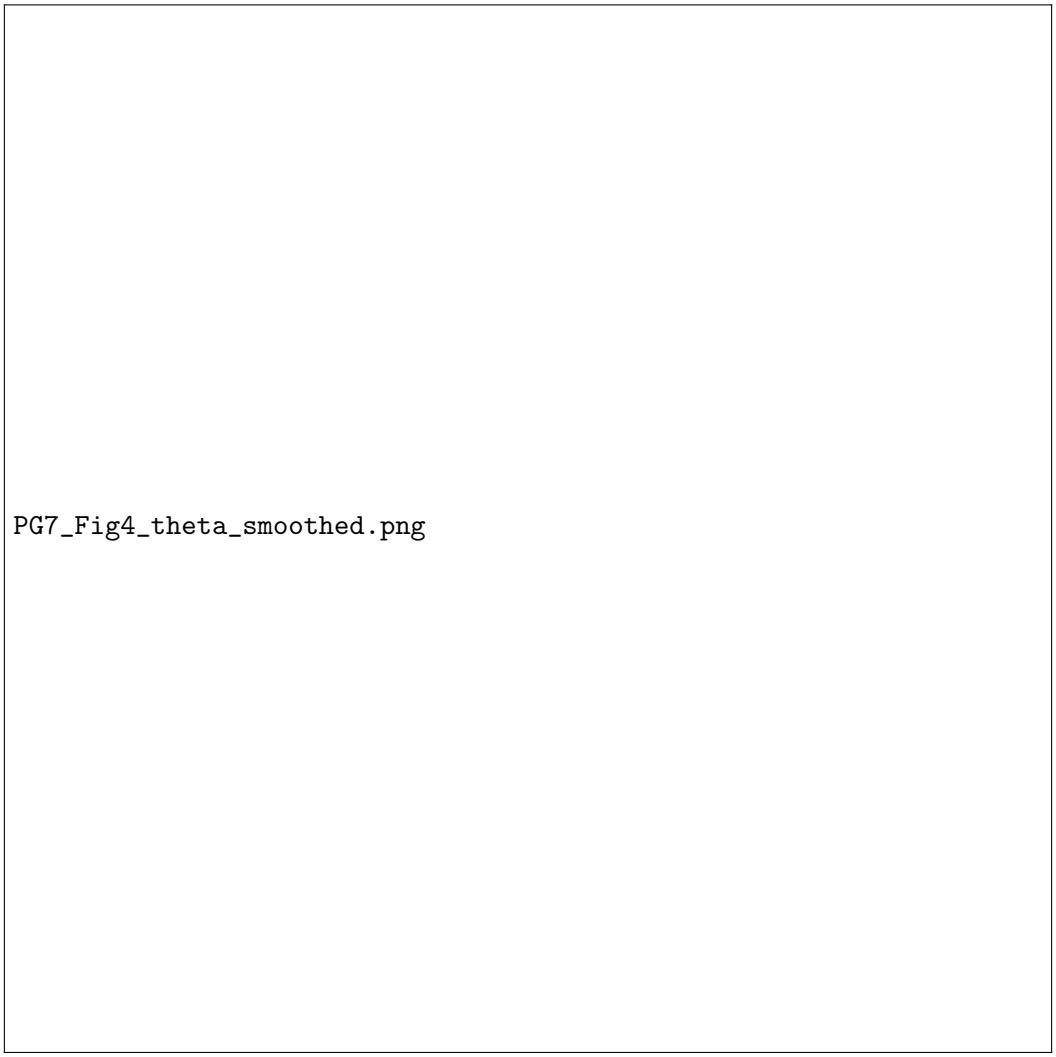

Figure 4: PG7 Fig. 4. Smoothed third-order functional $\Theta_n^{(W)}$ for several window sizes. Extended sign-persistent regions reflect higher-order coherence in curvature evolution.

This reveals a striking phenomenon:

Higher-order smoothness persists across thousands of indices.

6.4 Relation to curvature transitions

Using the identity

$$\Theta_n = (g_{n+3} - g_{n+2}) - 2(g_{n+2} - g_{n+1}) + (g_{n+1} - g_n),$$

we rewrite

$$\Theta_n = (g_{n+3} - g_{n+1}) - (g_{n+2} - g_n).$$

Since

$$g_{k+2} - g_k = \chi_k(g_k + g_{k+1}),$$

we obtain

$$\Theta_n = \chi_{n+1}(g_{n+1} + g_{n+2}) - \chi_n(g_n + g_{n+1}).$$

Thus Θ_n measures the difference between two consecutive curvature contributions. This confirms:

Θ_n is the discrete derivative of curvature (weighted by scale).

Large $|\Theta_n|$ correspond to curvature transitions—the same events that generate angle "kinks" in PG6.

6.5 Interpretation: higher-order stability

The suppression of $|\Theta_n|$ indicates that curvature evolves smoothly and rarely changes abruptly. Combined with the balance law of Section 4, this yields a higher-order structural principle:

Prime gaps minimize global roughness across first, second, and third orders.

This higher-order smoothness is a defining feature of the *Prime Geometry Attractor* developed in Section 6.

7 The Prime Geometry Attractor in State Space

Prime gap evolution can be viewed through the lens of the geometric state vector

$$X_n = (g_n,\ g_{n+1},\ \chi_n).$$

PG1–PG6 showed that each coordinate is highly constrained: g_n grows slowly, χ_n is small and sign-coherent, and the recurrence $g_{n+2} = g_n + \chi_n(g_n + g_{n+1})$ prevents abrupt second-order variation.

In PG7 we show that the *joint* evolution of (g_n, g_{n+1}, χ_n) is confined to a narrow region of $\mathbb{R}^3$ that acts as a **dynamical attractor**.

7.1 The dynamical state space

Consider the point cloud

$$\mathcal{S} = \{(g_n,\ g_{n+1},\ \chi_n) : n \le N\}.$$

For large N (millions of primes), visualizing $\mathcal{S}$ reveals:

- a narrow tube-like region elongated along (g_n, g_{n+1}),
- a tightly compressed thickness in the χ_n direction,
- curvature "sheets" corresponding to coherence phases,
- mild twisting corresponding to curvature sign changes.

This structure persists across many scales and remains stable under permutations of the sampling window.

Figure 5 illustrates this geometry.

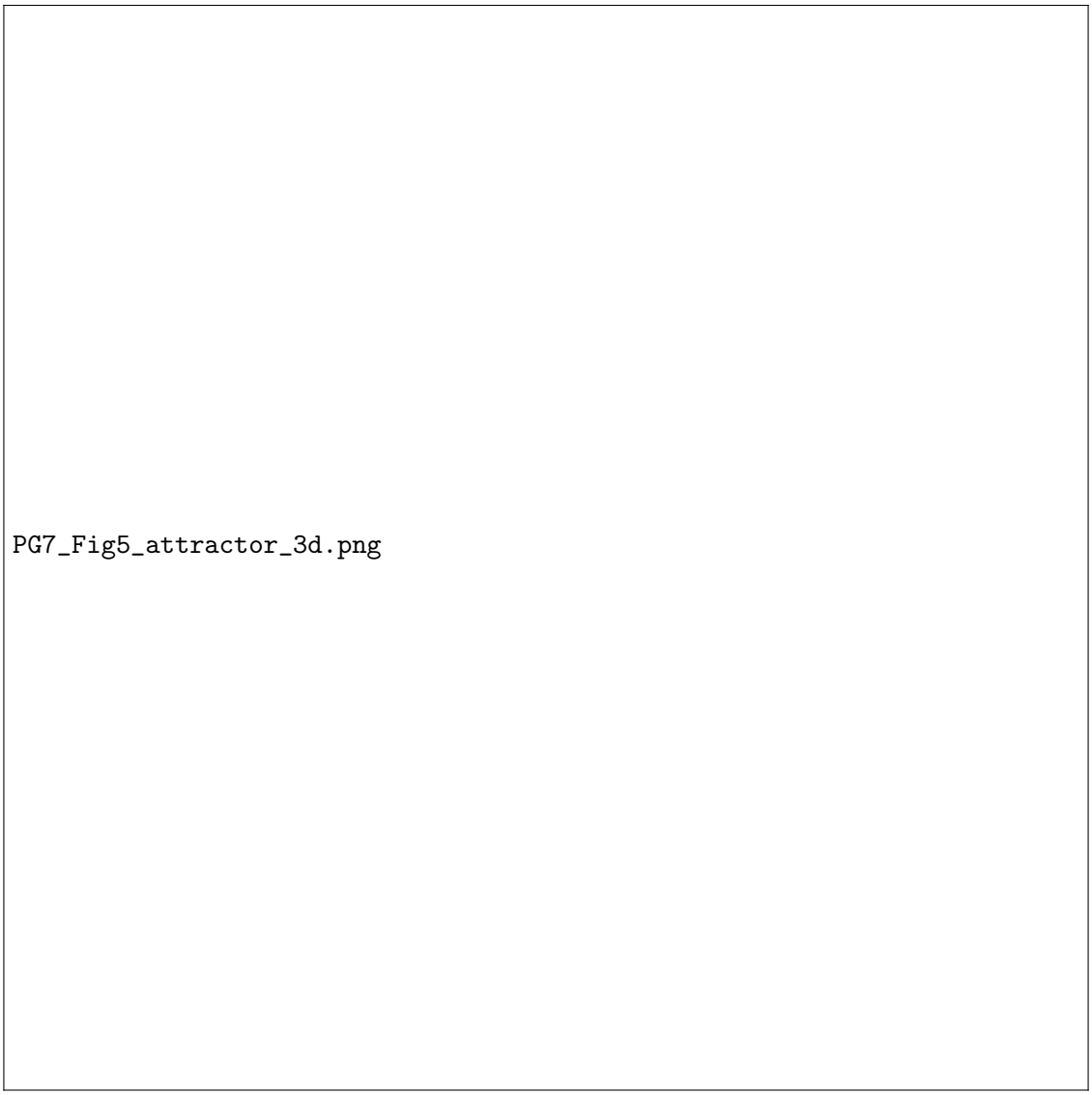

Figure 5: PG7 Fig. 5. The Prime Geometry Attractor in (g_n, g_{n+1}, χ_n)–space. Prime evolution occupies a narrow, tube-like manifold sharply distinct from the spread produced by random permutations.

7.2 Contrast with randomized models

If we randomize the gap multiset while preserving the values $\{g_n\}$, the resulting state cloud:

- fills a thick 3D volume,
- exhibits large excursions in χ_n,
- displays no coherent sheets or tubes,
- and shows no stability of orientation.

The true primes occupy less than a few percent of this volume. This separation persists even after projecting to pairs:

$$(g_n, g_{n+1}), \qquad (g_n, \chi_n), \qquad (g_{n+1}, \chi_n).$$

Thus the attractor is not an artifact of 3D visualization: *it is intrinsic to the geometric structure of the prime sequence.*

7.3 The attractor as a manifestation of geometric constraints

The attractor emerges naturally from:

- the recurrence (PG3),
- curvature suppression (PG2, PG4),
- coherence phases (PG4),
- angle drift coupling (PG5, PG6),
- the balance law (PG7 Section 4),
- and third-order smoothness (Section 5).

Each constraint restricts one projection of the state space; together they confine the entire trajectory to a stable manifold.

Prime gaps evolve on a dynamically stable manifold defined by curvature, angle drift, and high-or

We now formalize this as the *Prime Geometry Attractor*.

7.4 Definition (Prime Geometry Attractor)

Let $\mathcal{A}$ denote the smallest closed subset of $\mathbb{R}^3$ for which:

$$(g_1, g_2, \chi_1),\ (g_2, g_3, \chi_2),\ (g_3, g_4, \chi_3),\ \cdots \in \mathcal{A},$$

and such that

$$\|X_{n+1} - X_n\| \quad \text{is uniformly bounded relative to the local gap scale.}$$

Empirically $\mathcal{A}$ is a one-dimensional manifold with thickness that decays where curvature suppression is strongest.

8 Global Dynamics of Prime Evolution

We now integrate the results from Sections 3–6 into a unified dynamical picture. Prime gaps behave not as a random walk or renewal process but as a *smoothly evolving geometric dynamical system* governed by three principles.

8.1 Principle 1: Stability of the Prime Triangle angle

From the stability inequality,

$$\left|\alpha_n - \frac{\pi}{4}\right| \ll \sum_{k<n} \frac{|\chi_k|}{p_k},$$

and from curvature suppression,

$$|\chi_n| \ll 1 \quad \text{on most indices},$$

we obtain global stability.

The angle remains near equilibrium because curvature is globally small.

Thus the geometric orientation of the prime gaps evolves with near-constant slope.

8.2 Principle 2: Balance of expansion and contraction

From the balance law,

$$\sum_{k=n}^{m-1} \chi_k(g_k + g_{k+1}) = g_{m+1} - g_{n+1},$$

the cumulative signed curvature behaves like a conserved quantity:

- expansion phases (positive curvature)
- contraction phases (negative curvature)

cancel over long intervals. This prevents runaway divergence of the gap sequence.

8.3 Principle 3: Higher-order smoothness of curvature evolution

The third-order functional

$$\Theta_n = g_{n+3} - 3g_{n+2} + 3g_{n+1} - g_n$$

is sharply suppressed compared with randomized models.

Curvature itself evolves smoothly, with rare and modest transitions.

This acts as a "damping" mechanism on how curvature can change from one coherence phase to the next.

8.4 Synthesis: a low-dimensional geometric flow

Combining the three principles yields a global geometric dynamical system:

$$X_{n+1} = F(X_n) \qquad \text{with} \qquad X_n = (g_n,\, g_{n+1},\, \chi_n),$$

where F is constrained by:

- curvature recurrence,
- stability of angle,

- curvature balance,
- third-order smoothness.

The trajectory (X_n) therefore evolves along the attractor $\mathcal{A}$ rather than filling the ambient space.

Prime evolution is a smooth, coherence-driven flow on the Prime Geometry Attractor.

8.5 Implications

This global dynamical perspective explains:

- the persistent smoothness of the gap sequence,
- the rarity of large curvature or third-order anomalies,
- the tight clustering of return maps (PG2, PG3),
- the stability of angle near $45°$,
- and the structured failures of continuation heuristics (PG6).

The attractor picture thus unifies the entire PG1–PG7 framework into a single geometric dynamical interpretation.

9 Outlook

Prime Geometry VII presents a global dynamical interpretation of prime-gap evolution. Several natural directions arise from the attractor picture and the higher-order constraints identified here.

9.1 (1) Spectral analysis of the third-order functional

The smoothness and suppression of Θ_n suggest a structured spectral signature. Applying:

- Welch PSD methods,
- wavelet transforms,
- multi-resolution harmonic decompositions,

may reveal frequency bands or coherence scales not visible in χ_n alone. This would parallel and extend the spectral discoveries of PG5.

9.2 (2) Dynamical modeling of the attractor

A natural next step is to treat the mapping

$$X_n = (g_n, g_{n+1}, \chi_n), \qquad X_{n+1} = F(X_n),$$

as an empirical dynamical system. Fitting a phenomenological function F (local, nonlinear, low-dimensional) could enable:

- simulations that reproduce coherence phases,
- surrogate sequences matching higher-order smoothness,
- perturbation studies of attractor stability.

Such models would deepen the geometric view of prime evolution and may inform future theoretical approaches.

9.3 (3) Refined continuation heuristics

PG6 demonstrated that curvature+angle-based continuation almost works but fails in structured ways. PG7 indicates the missing ingredient:

$$\Theta_n \quad \text{and higher-order balance constraints.}$$

Future continuation heuristics incorporating third-order terms or attractor proximity conditions may substantially improve fidelity.

9.4 (4) Toward a unified manifold perspective

The attractor $\mathcal{A}$ may admit a more explicit description:

$$\mathcal{A} = \{X \in \mathbb{R}^3 : \Phi(X) = 0\},$$

for some empirically determined constraint function Φ. Understanding this manifold could unify PG1–PG7 into a single geometric theory and clarify the relationships among curvature, angles, action, and higher-order structure.

9.5 (5) Connections to zeta-zero geometry

PG5 and PG6 suggested resonances between prime curvature dynamics and certain zeta-zero difference signals. Applying the PG7 framework to analogous state variables for the zeta zeros (e.g., gap acceleration or curvature-like quantities) may uncover parallel attractor structures in the Riemann spectrum.

10 Conclusion

Prime Geometry VII extends the curvature and angle framework developed across PG1–PG6 into a global dynamical interpretation. The main insights are:

- **Stability of the Prime Triangle angle:** curvature suppression globally bounds deviation from 45°.

- **Higher-order balance:** signed curvature contributions cancel over long ranges, preventing runaway gap acceleration.
- **Third-order smoothness:** the functional Θ_n is sharply suppressed, revealing smooth evolution of curvature itself.
- **Prime Geometry Attractor:** the state sequence (g_n, g_{n+1}, χ_n) evolves along a narrow, low-dimensional manifold distinct from randomized models.

These features combine to produce a unified geometric dynamical system governing prime evolution. Rather than wandering freely through the space of all possible gap configurations, the prime sequence follows a stable, coherence-driven flow constrained by curvature, angle drift, and higher-order smoothness.

to global dynamics.**PG7 completes the transition from local geometry (PG1–PG6)**

to global dynamics.**PG7 completes the transition from local geometry (PG1–PG6)**

to global dynamics.**PG7 completes the transition from local geometry (PG1–PG6)**

to global dynamics.

This concludes the curvature-and-angle phase of the Prime Geometry series. The next papers (PG8 and beyond) will examine spectral refinement, manifold structure, and simulation-based models of the prime-gap attractor.